No Reference Color Image Contrast and Quality Measures

Karen Panetta, *Fellow*, IEEE, Chen Gao, *Student Member*, IEEE and Sos Agaian, *Senior Member*, IEEE

**Abstract — ***No-reference (NR) image quality assessment is essential in evaluating the performance of image enhancement and retrieval algorithms. Much effort has been made in recent years to develop objective NR grayscale and color image quality metrics that correlate with perceived quality evaluations. Unfortunately, only limited success has been achieved and most existing NR quality assessment is feasible only when prior knowledge about the types of image distortion is available. This paper present: a) a new NR contrast based grayscale image contrast measure: Root Mean Enhancement (RME); b) a NR color RME contrast measure CRME which explores the three dimensional contrast relationships of the RGB color channels; c) a NR color quality measure Color Quality Enhancement (CQE) which is based on the linear combination of colorfulness, sharpness and contrast. Computer simulations demonstrate that each measure has its own advantages: the CRME measure is fast and suitable for real time processing of low contrast images; the CQE measure can be used for a wider variety of distorted images. The effectiveness of the presented measures is demonstrated by using the TID2008 database. Experimental results also show strong correlations between the presented measures and Mean Opinion Score (MOS)*[1].

Index Terms — no reference (NR) measures, color contrast measure, color quality measure, Root Mean Enhancement (RME), Color Root Mean Enhancement (CRME), Color Quality Enhancement (CQE)

I. INTRODUCTION

Measuring the perceived quality of a color image is extremely difficult because human vision is highly nonlinear for different colors. In many practical applications, "no reference" color image quality assessment is desirable because the reference images may not always be available. Much effort has been made in recent years to develop objective image quality metrics that correlate with perceived quality measurements [1-6]. Unfortunately, only limited success has been achieved [7]. The most widely recognized method of determining color image quality is the subjective evaluation Mean Opinion Score (MOS). However, subjective evaluation is expensive with respect to time and resources, thus it is difficult to use in real time processing systems. The development of Computer Aided Design (CAD) made it desirable to formulate reliable objective color image quality measures. One would like to use such a measure that: (a) it is correlated with human perception; (b) it is reliable to monitor image quality for quality control systems [8]; (c) it is not limited to specific types of distortion; (d) it is independent of viewing distances; (e) it can be used to benchmark image processing algorithms [8]; (f) it can be embedded into image processing systems to assist selecting the optimal operating parameters [8]; and (g) it has low computational complexity and can be implemented in real-time.

In general, image quality measures can be classified into three categories: full reference (FR) approaches [1, 9-13], reduced reference (RR) approaches [14, 15] and no reference (NR) approaches [16-22]. FR approaches require the original image as the reference and determines the similarity between the distorted image and the reference image. However, in most practical cases, the cost of transmitting the original image is expensive, and the reference images may not always be available. RR metrics compare features of original and processed images and are more practical than FR metrics. However, they rely on auxiliary channels of information that may not always be present or affordable [23]. NR approaches, also called "blind" approaches, attempt "blindly" to make a judgment of image quality without prior knowledge of the reference images. Ideally, a NR measure could be the best choice for image quality assessment if it is applicable to all types of image distortions such as contrast changes, colorfulness degradation, compression artifacts, blurring effects and noise contamination. In practical applications, a "good" NR measure should also have strong correlation with human perception and low computational cost. Most existing grayscale NR measures are contrast-based or sharpness-based measures. Some methods use either Weber contrast [24] or Michelson contrast [16, 17]; some measures are based on kurtosis [18] or pixel derivatives [19]; some use the coefficients in DCT domain [20] or wavelet domain [21]. This article focuses on the development of NR color image measures.

The NR color image quality assessment is still a challenge. Most existing color image quality measures are proposed based on modifications of grayscale image quality measures. This is inspired by the observation that a color image is a three dimensional signal and each dimension can be seen as a grayscale image. Some existing methods apply grayscale measures on color images by converting the color image into a

[1] K. Panetta and C. Gao are with Department of Electrical and Computer Engineering, Tufts University, Medford, MA 02155 USA (email: Karen@ece.tufts.edu, Chen.Gao@tufts.edu)

S. Agaian is with Department of Electrical Engineering, University of Texas at San Antonio, San Antonio, TX 78249 USA (email: Sos.Agaian@utsa.edu).

Contributed Paper
Manuscript received 06/25/13
Current version published 09/25/13
Electronic version published 09/25/13.

grayscale image [1] or measuring the quality in each color component individually and then combining the measure values by different weights [25]. However, it is difficult to decide which optimal color model to use. Furthermore, the color to grayscale conversion is a lossy procedure. From this point of view, it is inappropriate to use traditional grayscale measures on a single plane of a color image. Due to these observations, a Color Root Mean Enhancement (CRME) measure is proposed in this paper. The CRME measure modifies grayscale measures, thus extending their applications to color images without converting the input color images into grayscale. The CRME measure is based on the root mean square contrast within and across color planes, thus the intra-plane structure and inter-plane colors are both considered in the image quality calculation.

Some other existing color image quality metrics focused on only one aspect of color image quality such as entropy [26, 27], brightness [28-30], colorfulness [5], sharpness [3, 21] and contrast [3]. Fu proposed a generic Color Image Quality Index (CIQI), which is formulated as a linear combination of colorfulness, sharpness and contrast metrics [4]. In this paper, another measure Color Quality Enhancement (CQE) is proposed. The CQE measure also linearly combines these three attributes using different metrics for colorfulness, sharpness and contrast.

This article provides new NR color image contrast and quality measures: CRME and CQE. The remainder of this paper is organized as follows: Section II reviews existing grayscale image quality assessment methods. Section III proposes a new root mean square based contrast measure RME for both grayscale and color images and proposes a method to extend the 2D grayscale image measures to 3D color image measures. Section IV introduces another measure, Color Quality Enhancement (CQE) by linearly combining colorfulness, sharpness and contrast into single color image quality expression. Section V presents the experimental results and comparisons to the existing color measure Color Image Quality Index (CIQI) [4] and Mean Opinion Score (MOS). An example of using the CRME and CQE measures to assist selecting optimal operating parameter is also shown in this section. The conclusions are discussed in Section VI.

II. NR Grayscale Contrast Measures

Since grayscale image measures can be used and extended to assess color image quality, it is necessary to review existing grayscale image contrast measures.

In the past, NR measures attempted to use statistical measures of the gray level distribution of local contrast enhancement. These include mean, variance, or entropy, but these approaches have not been particularly useful or meaningful. Some more sophisticated NR grayscale measures have been proposed [6, 8, 31, 32]. These methods focus on specific types of distortions like blurring, JPEG compression or JPEG2000 compression. Morrow et al. [33] introduced a measure based on the contrast histogram, which has a much greater consistency than statistical measures. Following this observation, several measures of image enhancement have been developed by using a contrast measure.

The Weber contrast is used to measure the local contrast of a single target of uniform luminance seen against a uniform background [34]. Developed by Agaian [35], the first practical measures, which are based on the Weber's law, were the Measure of Enhancement (EME) and Measure of Enhancement by Entropy (EMEE). Another commonly used contrast measure, Michelson contrast, measures the periodic pattern [34]. DelMarco and Agaian created a visibility map by extending the Michelson operator to two dimensions [36]. Then the Michelson-Law measure of enhancement (AME), and Michelson-Law measure of enhancement by entropy (AMEE) [16] are proposed based on the Michelson contrast and logarithmic processing. Since Parametric logarithmic image processing (PLIP) [37] operations have been shown to be consistent with characteristics of the human visual system and the nonlinear properties of image enhancement algorithms, Panetta et al. have developed the logarithmic Michelson contrast measure (logAME) and logarithmic AME by entropy (logAMEE) [17, 22, 38] by incorporating PLIP operations in AME and AMEE. To reduce the measure sensitivity to noise and steep edges, a second derivative based measure (SDME) was also introduced [19]. It measures the change ratio of the variation speed of pixel values and considers the center pixel value in addition to the local maximum and minimum value.

The definitions of these measures are listed in Table. I. A general model is provided in [35]. Users can select the coefficients and functions for their applications. Each of the measures has different physical explanations within it, so it is necessary to choose a proper measure for a specific image type and application.

III. NR Color Image Contrast Measure: Cube Root Mean Enhancement (CRME)

This section introduce a new enhancement measure using the concept of Root Mean Square (RMS) contrast and a new method to extend the regular grayscale image contrast measure to three dimensions so that it is applicable for measuring color image contrast.

A. New contrast measures in grayscale image

The existing measures are either based on the Weber contrast [24, 36] or Michelson contrast [16, 17]. As stated in the previous section, the Weber contrast is used to measure the local contrast of a single target seen against a uniform background, while the Michelson contrast is commonly used to measure the contrast of periodic pattern [34]. However, in complex images these uniformity or periodicity conditions are not always true. So a new method based on the RMS contrast which does not depend on spatial frequency content or distribution of contrast in the image is proposed in this section.

Regular RMS contrast is a pixel-wised contrast as defined in (1). The new Root Mean Enhancement measure (RME) incorporates the idea of RMS contrast and the Human Visual

TABLE I
EXISTING GRAYSCALE NR MEASURES

Grey Image Measure	Definition	Features
EME	$EME_{k_1k_2} = \frac{1}{k_1k_2}\sum_{k=1}^{k_1}\sum_{l=1}^{k_2} 20\ln(\frac{I_{\max,k,l}}{I_{\min,k,l}})$	Weber contrast based enhancement measure Applicable to uniform background images [24]
EMEE	$EMEE_{k_1k_2} = \frac{1}{k_1k_2}\sum_{k=1}^{k_1}\sum_{l=1}^{k_2} \alpha(\frac{I_{\max,k,l}}{I_{\min,k,l}})^{\alpha}\ln(\frac{I_{\max,k,l}}{I_{\min,k,l}})$	Weber contrast based enhancement measure Incorporate entropy in EME More randomness in image, the bigger α to choose [24]
Visibility	$Visibility = \sum_{k=1}^{k_1}\sum_{l=1}^{k_2}\frac{I_{\max,k,l}-I_{\min,k,l}}{I_{\max,k,l}+I_{\min,k,l}}$	Two dimensional Michelson contrast based measure [36]
AME	$AME_{k_1k_2} = -\frac{1}{k_1k_2}\sum_{k=1}^{k_1}\sum_{l=1}^{k_2} 20\ln(\frac{I_{\max,k,l}-I_{\min,k,l}}{I_{\max,k,l}+I_{\min,k,l}})$	Michelson contrast based enhancement measure Applicable to non-uniform images/ Applicable to Periodic background [16]
AMEE	$AME_{k_1k_2} = -\frac{1}{k_1k_2}\sum_{k=1}^{k_1}\sum_{l=1}^{k_2} \alpha(\frac{I_{\max,k,l}-I_{\min,k,l}}{I_{\max,k,l}+I_{\min,k,l}})^{\alpha}\ln(\frac{I_{\max,k,l}-I_{\min,k,l}}{I_{\max,k,l}+I_{\min,k,l}})$	Michelson contrast based enhancement measure Incorporate entropy in AME [16]
logAME	$\log AME_{k_1k_2} = \frac{1}{k_1k_2}\tilde{\otimes}\sum_{k=1}^{k_1}\sum_{l=1}^{k_2}\frac{1}{20}\ln(\frac{I_{\max,k,l}\tilde{\Theta}I_{\min,k,l}}{I_{\max,k,l}\tilde{\oplus}I_{\min,k,l}})$	PLIP version of AME/ More appealing to human vision [17, 22]
logAMEE	$\log AMEE_{k_1k_2} = \frac{1}{k_1k_2}\tilde{\otimes}\sum_{k=1}^{k_1}\sum_{l=1}^{k_2}\alpha(\frac{I_{\max,k,l}\tilde{\Theta}I_{\min,k,l}}{I_{\max,k,l}\tilde{\oplus}I_{\min,k,l}})^{\alpha}\ln(\frac{I_{\max,k,l}\tilde{\Theta}I_{\min,k,l}}{I_{\max,k,l}\tilde{\oplus}I_{\min,k,l}})$	PLIP version of AMEE/ More appealing to human vision [17, 22]
SDME	$SDME_{k_1k_2} = -\frac{1}{k_1k_2}\sum_{k=1}^{k_1}\sum_{l=1}^{k_2} 20\ln\left\lvert\frac{I_{\max,k,l}-2I_{center,k,l}+I_{\min,k,l}}{I_{\max,k,l}+2I_{center,k,l}+I_{\min,k,l}}\right\rvert$	Second derivative based measure, It is not sensitive to noise [19]
HVS Visibility	$Visibility_{HVS} = \frac{\sum_{i=1}^{n} a_i \tilde{\otimes} G_i(\frac{F_i(MF_{i1})}{F_i(MF_{i2})})^{n_i}\tilde{\oplus} b_i \tilde{\otimes} G_i(\frac{F_i(MF_{i3})}{F_i(MF_{i4})})^{n_i}}{\sum_{j=1}^{n} c_j \tilde{\otimes} L_j(\frac{F_j(MF_{j1})}{F_j(MF_{j2})})^{m_j}\tilde{\oplus} d_j \tilde{\otimes} L_j(\frac{F_j(MF_{j3})}{F_j(MF_{j4})})^{m_j}}$	A general visibility model [35]

System (HVS) properties. It measures the relative RMS contrast in the log domain. The RME measure is expressed in (2). The image is divided into k_1k_2 blocks, $I_{i,j}$ is the center pixel intensity in block i, j, $\frac{I_1+I_2+...+I_n}{n}$ is the average intensity in block i, j and n is the total number of pixel within each block. It is worth noting that $\log\left\lvert I_{i,j}-\frac{I_1+I_2+...+I_n}{n}\right\rvert$ returns a negative value if the difference between the center and its neighbors is smaller than 1. Practically, $\max(1,\left\lvert I_{i,j}-\frac{I_1+I_2+...+I_n}{n}\right\rvert)$ is used to make sure the RME is always positive thus is proportional to the difference.

$$C_{RMS} = \sqrt{\frac{1}{MN}\sum_{i=0}^{M-1}\sum_{j=0}^{N-1}(I_{i,j}-\bar{I})^2} \qquad (1)$$

$$RME = \frac{1}{k_1k_2}\sqrt{\sum_{i=1}^{k_1}\sum_{j=1}^{k_2}\left\lvert\frac{\log\left\lvert I_{i,j}-\frac{I_1+I_2+...+I_n}{n}\right\rvert}{\log\left\lvert I_{i,j}+\frac{I_1+I_2+...+I_n}{n}\right\rvert}\right\rvert} \qquad (2)$$

When the center pixel has an intensity value approximately equal to the average value of the current block, the contrast is small. Thus, the RME measure is small for low contrast images and vice versa for images with high contrast. The recommended block size is 3x3 and no larger than 5x5 because image statistical features are spatially non-stationary and image distortion is also space variant.

B. New contrast measure in color image

A color image is a multi-spectral signal, and therefore it is reasonable to expand the traditional formulation of grayscale contrast measures so that it can be used to measure the multidimensional color image contrast. To be more specific, the contrast measures can be performed not only within each color plane but also across color planes. The cross-plane contrast models the differences between color planes and reveals the color variation and structural differences raised from different color components. Based on this idea, the Color/Cube RME (CRME) is proposed to measure the relative difference of the color cube center and all the neighbors in the current color cube.

$$CRME = \frac{1000}{k_1k_2}\sqrt{\sum_{i=1}^{k_1}\sum_{j=1}^{k_2}\left\lvert\frac{\log\left\lvert I_{i,j}-\sum_{c=1}^{3}\lambda_c\frac{I_{c1}+I_{c2}+...+I_{cn}}{n}\right\rvert}{\log\left\lvert I_{i,j}+\sum_{c=1}^{3}\lambda_c\frac{I_{c1}+I_{c2}+...+I_{cn}}{n}\right\rvert}\right\rvert^{\alpha}} \qquad (3)$$

In the implementation, the intensity value of the center pixel is used as the cube center pixel intensity. λ_c represents the weights for different color components. In this article, $\lambda_r = 0.299$, $\lambda_g = 0.587$ and $\lambda_b = 0.114$ are used in accordance with the NTSC standard. According to the Human

Visual System (HVS) properties [39], human eyes are not equally sensitive to the Just Noticeable Difference (JND). To compensate for this, an α power is assigned to the ratio based on the region to which the local background of the current cube belongs. If it belongs to the DeVries-Rose region, α=0.2; if it belongs to the Weber region, α=0.4; and if the background intensity falls into the Saturation region, α=0.8.

IV. NR Color Image Quality Measure: Color Quality Enhancement (CQE)

Next, another color image quality measure CQE is introduced. CQE uses a polling method to combine chrominance information with sharpness and contrast. The idea is similar to the CIQI measure [4] but differs in many ways. The algorithm described in [4] is implemented and it is observed that their attribute metrics do not have strong correlations with human visual perceptions. Thus different colorfulness, sharpness and contrast metrics are used in the CQE measure. The block diagram of the CQE measure is shown in Fig. 1.

$$CQE = c_1 \times colorfulness + c_2 \times sharpness + c_3 \times contrast \quad (4)$$

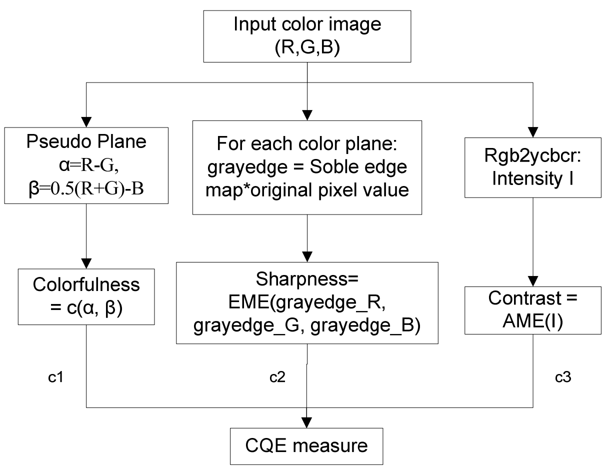

Fig. 1. Block diagram of the CQE measure

Colorfulness is the attribute of chrominance information humans perceive. Hasler and Susstrunk have shown that the colorfulness can be represented effectively with combinations of image statistics [5]. The CIQI measure [4] uses the colorfulness metric similar to [5] but normalizes the dynamic range to 0 and 1. The CIQI colorfulness metric is shown in (5), where $\alpha = R-G$ and $\beta = 0.5(R+G)-B$ are opponent red-green and yellow-blue spaces, σ_α^2 , σ_β^2 , μ_α , μ_β represent the variance and mean values along these two opponent color axes as defined in (6) and (7).

$$CIQI\_colorfulness = \left(\sqrt{\sigma_\alpha^2 + \sigma_\beta^2} + 0.3\sqrt{\mu_\alpha^2 + \mu_\beta^2}\right) / 85.59 \quad (5)$$

$$\mu_\alpha = \frac{1}{N}\sum_{p=1}^{N} \alpha_p \quad (6)$$

$$\sigma_\alpha^2 = \frac{1}{N}\sum_{p=1}^{N} (\alpha_p^2 - \mu_\alpha^2) \quad (7)$$

It is observed that with this expression, the metric value does not linearly correspond to human perceptions. Thus, it is reasonable to introduce the logarithmic operation into the colorfulness measure because the subjective sensation is proportional to the logarithm of the stimulus. In the CQE measure, two image colorfulness metrics are proposed by combinations of a subset of color image quantities in the logarithmic domain. Equation (8) formulates the ratio of the variance to the average chrominance in each of the opponent component. Equation (9) takes the logarithmic operation first and then calculates the relative variance and mean over the entire chrominance spaces. Both formulations have good correlation with human perception. Fig. 2 shows the sensitivity of the colorfulness metrics. Fig. 2 (a) is a reference image from TID2008 database [40] and (b)-(d) are obtained by linearly reducing chrominance in the CIELab color space. The image characteristics for the four images in Fig.2 are shown in Table. II. In this paper, the $colorfulness^1$ metric is used for the calculation of the CQE measure for the reason that it does not introduce extra variables other than the variance and mean of each color component.

$$colorfulness^1 = 0.02 \times \log\left(\frac{\sigma_\alpha^2}{|\mu_\alpha|^{0.2}}\right) \times \log\left(\frac{\sigma_\beta^2}{|\mu_\beta|^{0.2}}\right) \quad (8)$$

$$colorfulness^2 = 0.02 \times \frac{\log\sigma_\alpha^2 \times \log\sigma_\beta^2}{\log\sigma_c^2} \times \frac{\log\mu_\alpha^2 \times \log\mu_\beta^2}{\log\mu_c^2} \quad (9)$$

$$\mu_c = \frac{1}{2N}\left(\sum_{p=1}^{N} \alpha_p + \sum_{p=1}^{N} \beta_p\right) \quad (10)$$

$$\sigma_c^2 = \frac{1}{2N}\left(\sum_{p=1}^{N} (\alpha_p^2 - \mu_c^2) + \sum_{p=1}^{N} (\beta_p^2 - \mu_c^2)\right) \quad (11)$$

TABLE II
Image Characteristics for Four Images with Different Colorfulness Degradations in Fig. 2

Image characterestics	Fig. 2 - (a)	Fig. 2 - (b)	Fig. 2 - (c)	Fig. 2 - (d)
μ_α	14.0491	11.0594	6.9963	3.8446
μ_β	45.9446	35.6368	22.6421	12.0858
σ_α	41.5464	28.5843	16.2527	8.0910
σ_β	54.3328	43.1891	27.9355	15.2065

Sharpness is the attribute related to the preservation of fine details and edges. In our method, the Sobel edge detection algorithm is first applied on each RGB color component and then, the binary edge map is multiplied with the original values to obtain three grayscale edge maps. Since sharpness is proportional to the perceived steepness of slopes, it is reasonable to treat each of the grayscale edge maps as an input image and measure the Weber contrast if the window size is small enough. In this article, the Weber contrast based Measure of Enhancement EME [24] is used on each grayscale edge map with an overlapped window size 3x3. It is worth noticing that if the input image is a JPEG compressed image, the window which is overlapped with JPEG artifact block borders will be discarded. Fig. 3 shows the sensitivity of the sharpness metrics for Gaussian blur images in TID2008 database [40]. The CIQI [4] measure shows that the image in Fig. 3 (c) has better sharpness than the image in Fig. 3 (a), which is not corresponding to human observation. The CQE measure correctly ranks the image sharpness.

	(a)	(b)	(c)	(d)
CIQI_colorfulness	0.9675	0.7359	0.4607	0.2457
CQE_colorfulness	1.0006	0.8487	0.6262	0.3869
CQE_colorfulness	0.9021	0.7547	0.5279	0.2955

Fig. 2. Image results on the sensitivity of colorfulness metrics. (a)-(d) are four images with different levels of colorfulness distortions.

	(a)	(b)	(c)	(d)
CIQI_sharpness	***0.1201***	0.1031	***0.1412***	0.0747
CQE_sharpness	1.2747	0.8990	0.6279	0.4640

Fig. 3. Image results on the sensitivity of sharpness metrics. (a)-(d) are four images with different levels of sharpness distortions. Visually, (a) has better sharpness than (c). However, the CIQI sharpness metric disobeys the obseravtion.

	(a)	(b)	(c)	(d)
CIQI_contrast	***0.6812***	***0.7664***	0.3453	0.1785
CQE_contrast	0.9297	0.7529	0.5972	0.5388

Fig. 4. Image results on the sensitivity of contrast metrics. (a)-(d) are four images with different levels of contrast distortions. Visually, (a) has better contrast than (b). However, the CIQI sharpness metric disobeys the obseravtion.

$$sharpness = \sum_{c=1}^{3} \lambda_c EME_{sharpness}(grayedge_c) \tag{12}$$

$$EME_{sharpness} = \frac{2}{k_1 k_2} \sum_{l=1}^{k1} \sum_{k=1}^{k_2} \log\left(\frac{I_{\max,k,l}}{I_{\min,k,l}}\right) \tag{13}$$

The Michelson-Law measure of enhancement AME has been proven to be effective in evaluating grayscale image contrast [16]. A similar method is adopted to measure the contrast by applying the AME measure in the intensity component. The original AME expression returns smaller values for images with larger contrast. Therefore, a power of -0.5 is added to each term so that the better contrast image has a larger contrast metric value. Fig. 4 shows the sensitivity of the contrast metrics for contrast changed images in the TID2008 database [40]. The CIQI [4] measure shows that the image in Fig. 4 (b) has better contrast than the image in Fig. 4 (a), which disobeys human observation. The CQE measure correctly ranks the image contrast.

$$contrast = AME_{contrast}(Intensity) \tag{14}$$

$$AME_{contrast} = \frac{1}{k_1 k_2} \sum_{l=1}^{k_1} \sum_{k=1}^{k_2} \left(\log\left(\frac{I_{\max,k,l} + I_{\min,k,l}}{I_{\max,k,l} - I_{\min,k,l}}\right)\right)^{-0.5} \tag{15}$$

After the colorfulness, sharpness and contrast metrics are obtained, a multiple linear regression (MLR) on 48 training images from TID2008 database is applied to obtain the three coefficients in (4). It is observed that the colorfulness, sharpness and contrast are calculated independently so the three attributes can be parallel processed to accelerate operating speed. For an image with a specific type of distortion, the CQE measure achieves better performance if the training set has the same distortion. For images with unknown distortions, a generic set of coefficients can be used. The recommended coefficients for some types of distortions and for generic usage are listed in Table. III.

TABLE III
RECOMMENDED LINEAR COMBINATION COEFFICIENTS FOR CQE MEASURES. THE COEFFICIENTS ARE BTAINED BY APPLYING MLR ON 48 TRAINING IMAGES SUFFERING FROM THE CORRESPONDING DISTORTIONS.

Distortion Type	c1	c2	c3
Gaussian blur	0.2736	0.2261	0.5003
Contrast change	0.4358	0.1722	0.3920
JPEG2000 compression	0.2170	0.7100	0.0731
Denoising	0.5002	0.2448	0.2549
Generic distortions	0.2946	0.3483	0.3571

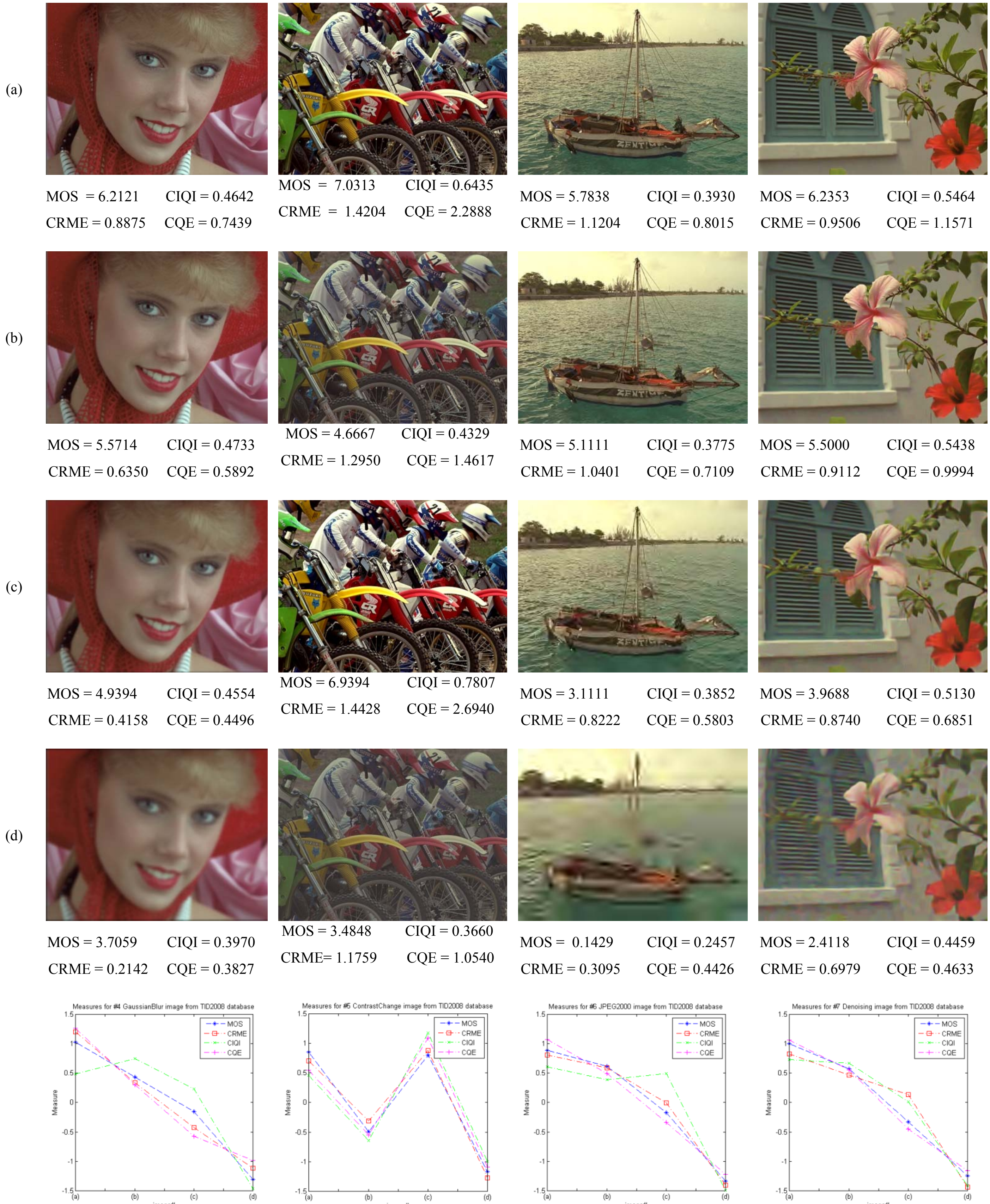

(1) (2) (3) (4)

Fig. 5. Comparisons of measure metrics for images suffer from different levels of distortions. (1) Portait: Gaussian blurred images, (2) Bycicle: Contrast change images, (3) Boat: JPEG2000 compressed images and (4) Flower: Denoised images. Row (a)-(d) are four levels of distortions. All measure values are normalized for better visual comparison.

V. Experimental Results

The TID2008 database [40] is a published benchmark for measuring color image qualities and it is used in this paper to test the effectiveness of the color measures. It is worth noting that since the measures have different dynamic ranges, all measure values are normalized for comparison purposes.

Some most common correlation coefficients are used to analyze the statistical relationship between two sets of images. Pearson's product moment correlation measures how far each measure value deviates from the MOS [41]. Spearman's rank order correlation compares the rank of image qualities and Kendall's tau correlation is usually suggested for non-normal data [42]. Table. IV summarizes the three average correlations for four types of distorted images in the TID2008 database. The results show that the proposed two measures have good correlation with MOS on the order 0.90 and performance range from 0.65 to 47.22 percent better than CIQI [4].

The color image quality measures can be used to rank image qualities. Some images with different levels of distortions and the corresponding measure values are shown in Fig. 5. It is observed that the CRME and CQE metrics have strong correlation with the MOS. The four testing images suffer from different types of distortions: The portrait images are distorted by Gaussian blurring, the bicycle images have different contrast, the boat images are JPEG2000 compressed images and flower images are processed by denoising filters. For these images, the coefficients obtained from training images that exhibit the same type of distortions in Table. III are used.

TABLE IV

COMPARISON OF MEASURE METRICS IN ACCORDANCE WITH AVERAGE PEARSON, SPEARMAN AND KENDALL CORRELATION WITH MOS ON FOUR TYPES OF DISTORTIONS: GAUSSIAN BLUR, CONTRAST CHANGE, JPEG2000 COMPRESSION, DENOISING IN TID2008 DATABASE

Distortion Type	Measure	SampleSize /number of Simulations	PRCC	SRCC	KRCC
Gaussian Blur	CRME	48/100	0.9882	1.0000	1.0000
	CIQI		0.6527	0.5833	0.5278
	CQE		0.9631	1.0000	1.0000
Contrast change	CRME	48/100	0.9569	0.8333	0.7500
	CIQI		0.9099	0.8167	0.7222
	CQE		0.9164	0.8333	0.7500
JPEG2000 compression	CRME	48/100	0.9891	1.0000	1.0000
	CIQI		0.6945	0.7667	0.6944
	CQE		0.9255	0.9833	0.9722
Denoising	CRME	48/100	0.8999	0.9000	0.8611
	CIQI		0.6616	0.5667	0.5278
	CQE		09942	1.0000	1.0000

Fig. 6 shows JPEG compressed house images. However, the coefficients for this type of distortion are not given in Table III. Here, the generic distortion coefficients are used. The results in Fig. 6 show that despite the JPEG compression images not specifically being trained by using the images with the same distortion, the genetic coefficients performs well.

The measures can also be used for assisting in the selection of optimal operating parameters for image enhancement, denoising or decompression algorithms. Fig. 7 shows an example of applying the power law on each color component of an under illuminated image. For dark images, the power α should be smaller than 1. For the test image in Fig. 7, the CRME and CQE both independently selected the optimal alpha power at 0.5 and 0.55 and both achieve good enhancement results with the selected parameters. Fig. 7 also shows enhancement results with other α values. Smaller alpha values tends to show a color casting problem and greater alpha values do not work for the under illumination image.

MOS = 6.0625 CIQI = 0.3525

CRME = 1.3577 CQE = 0.7647

(a)

MOS = 5.0000 CIQI = 0.3519

CRME = 1.3081 CQE = 0.7006

(b)

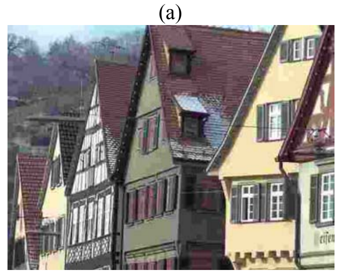

MOS = 3.3226 CIQI = 0.3483

CRME = 1.2222 CQE = 0.5863

(c)

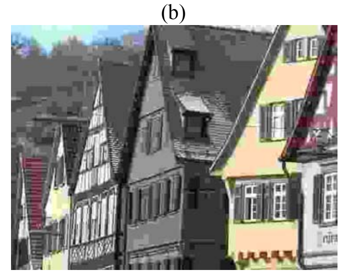

MOS = 1.0938 CIQI = 0.3257

CRME = 1.0935 CQE = 0.4868

(d)

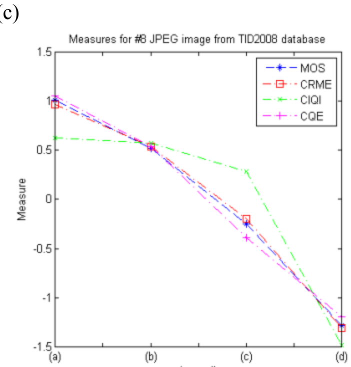

(e)

Fig. 6. (a)-(d) JPEG house images suffer from different levels of distortions. (e) The measure metrics for the corresponding images. All measure values are normalized for better visual comparison.

Table. V shows the average execution time for 48 test images. The size of the test images is 512 by 384 by 3. The testing computer features 2.66GHz frequency CPU and 3.25GB RAM. Each simulation is repeated 100 times. The simulation results show that the CRME has fastest execution speed. Besides, the CRME measure does not require training procedures thus is applicable for real-time applications if the

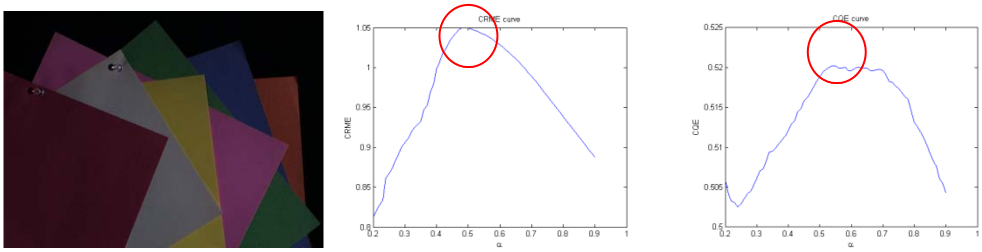

Original image | CRME curve | CQE curve

Enhancement with α=0.1 | Enhancement with α=0.5 (CRME optimal parameter) | Enhancement with α=0.55 (CQE optimal parameter) | Enhancement with α=0.9

Fig. 7. Using CRME and CQE for assisting selecting optimal alpha power for an underillminated image.

test image suffers from low frequency distortions. The CQE measure requires 2.1 times running time than the CRME measure. However, since the CQE does not only measure the contrast, but also combines colorfulness and sharpness metrics in addition to contrast metric, it is applicable to a wider variety of distorted images.

TABLE V
AVERAGE EXECUTION TIME FOR THE CRME, CQE AND CIQI MEASURES OF 100 SIMULATIONS

	CRME	CQE	CIQI
Average execution time (second)	0.4395	0.9272	0.5085

VI. CONCLUSIONS

NR color image quality assessment is essential in evaluating the performance of color image processing algorithms, especially when the reference images are not accessible. In this article two new NR color measures are presented: a color contrast measure CRME and a color quality measure CQE. Our results indicate that the CRME measure has fast processing time, which makes it applicable for real time image processing systems. While the CQE quality measure is composed of sharpness, colorfulness and contrast attributes, it has the advantage of being applicable to a wider variety of distorted images. For images suffering from low frequency distortions, both measures are reliable to evaluate image quality. The CRME and CQE with CIQM and MOS in 500 images from the TID2008 image quality database are compared. Experimental results showed that both new measures have good correlation with MOS, and they can be used to assist in the selection of optimal operating parameters for image processing algorithms.

REFERENCES

[1] Z. Wang, A. C. Bovik, H. R. Sheikh, and E. P.Simoncelli, "Image Quality Assessment: From Error Visibility to Structural Similarity," IEEE Transactions on Image Processing, vol. 13, April, 2004.

[2] S. Süsstrunk and S. Winkler, "Color image quality on the Internet," Proc. SPIE/IS&T Internet Imag, vol. 5304, pp. 118-131, 2004.

[3] B. Bringier, N. Richard, M. C. Larabi, and C. Fernandez-Maloigne, "No-reference perceptual quality assessment of colour image," in Proceedings of the European Signal Processing Conference (EUSIPCO'06), 2006.

[4] Y.-Y. Fu, "Color image quality measures and retrieval," PhD thesis, Department of Computer Science, New Jersey Institute of Technology, January 2006.

[5] D. Hasler and S. E. Suesstrunk, "Measuring colorfulness in natural images," in Electronic Imaging 2003, 2003, pp. 87-95.

[6] R. Sakuldee, N. Yamsang, and S. Udomhunsakul, "Image quality assessment for JPEG and JPEG2000," in Convergence and Hybrid Information Technology, 2008. ICCIT'08. Third International Conference on, 2008, pp. 320-325.

[7] Z. Wang, A. C. Bovik, and L. Lu, "Why is image quality assessment so difficult?" in Acoustics, Speech, and Signal Processing (ICASSP), 2002 IEEE International Conference on, 2002, pp. IV-3313-IV-3316.

[8] Z. Wang, H. R. Sheikh, and A. C. Bovik, "No-reference perceptual quality assessment of JPEG compressed images," in Image Processing. 2002. Proceedings. 2002 International Conference on, 2002, pp. I-477-I-480 vol. 1.

[9] D. Chandler and S. Hemami, "VSNR: A Wavelet-Based Visual Signal-to-Noise Ratio for Natural Images," IEEE Transactions on Image Processing, vol. 16, September, 2007.

[10] E. A. Silva, K. Panetta, and S. S. Agaian, "Quantifying image similarity using measure of enhancement by entropy," Mobile Multimedia/Image Processing for Military and Security Applications, vol. 6579, p. 65790U, 2007.

[11] S. Nercessian, S. Agaian, and K. Panetta, "An Image Similarity Measure Using Enhanced Human Visual System Characteristics," in Mobile Multimedia/Image Processing, Security, and Applications, 2011.

[12] Z. Wang and A. C. Bovik, "Mean squared error: love it or leave it? A new look at signal fidelity measures," Signal Processing Magazine, IEEE, vol. 26, pp. 98-117, 2009.

[13] H.-S. Han, D.-O. Kim, and R.-H. Park, "Structural information-based image quality assessment using LU factorization," IEEE Transactions on Consumer Electronics, vol. 55, pp. 165-171, 2009.

[14] Q. Li and Z. Wang, "General-purpose reduced-reference image quality assessment based on perceptually and statistically motivated image

representation," in Image Processing, 2008. ICIP 2008. 15th IEEE International Conference on, 2008, pp. 1192-1195.
[15] S. Wolf and M. H. Pinson, "Spatial-temporal distortion metric for in-service quality monitoring of any digital video system," in Photonics East'99, 1999, pp. 266-277.
[16] S. S. Agaian, B. Silver, and K. A. Panetta, "Transform coefficient histogram-based image enhancement algorithms using contrast entropy," IEEE Transactions on Image Processing, vol. 16, pp. 741-758, 2007.
[17] K. Panetta, E. Wharton, and S. Agaian, "Human visual system-based image enhancement and logarithmic contrast measure," IEEE Transactions on Systems, Man, Cybernetics, vol. 38, Feb. 2008.
[18] J. Caviedes and F. Oberti, "A new sharpness metric based on local kurtosis, edge and energy information," Signal Processing: Image Communication, vol. 19, pp. 147-161, 2004.
[19] Y. Zhou, K. Panetta, S. Agaian, and H. Jia, "Nonlinear unsharp masking for mammogram enhancement," IEEE Transactions on Information Technology in Biomedicine, vol. 15, pp. 918-928, November, 2011.
[20] J. Tang, E. Peli, and S. Acton, "Image enhancement using a contrast measure in the compressed domain," IEEE Signal Processing Letters, vol. 10, pp. 289-292, 2003.
[21] A. Maalouf and M.-C. Larabi, "A no reference objective color image sharpness metric," in EUSIPCO, 2010, pp. 1019-1022.
[22] E. Wharton, K. Panetta, and S. Agaian, "A logarithmic measure of image enhancement," in Mobile Multimedia/Image Processing for Military and Security Applications, 2006.
[23] N. Suresh, R. Palaniappan, P. Mane, and N. Jayant, "Testing of a no-reference VQ metric: Monitoring quality and detecting visible artifacts," in Proceedings of the Fourth International Workshop on Video Processing and Quality Metrics for Consumer Electronics, 2009.
[24] S. S. Agaian, K. P. Lentz, and A. M. Grigoryan, "A new measure of image enhancement," in IASTED International Conference on Signal Processing & Communication, 2000, pp. 19-22.
[25] C. Gao, K. Panetta, and S. Agaian, "A new color contrast enhancement algorithm for robotic applications," in IEEE conference on Technologies for Practical Robot Applications, 2012.
[26] Y. Wang, Q. Chen, and B. Zhang, "Image enhancement based on equal area dualistic sub-image histogram equalization method," IEEE Transactions on Consumer Electronics, vol. 45, pp. 68-75, 1999.
[27] M. Kim and M. Chung, "Recursively separated and weighted histogram equalization for brightness preservation and contrast enhancement," IEEE Transactions on Consumer Electronics, vol. 54, pp. 1389-1397, 2008.
[28] S.-D. Chen and A. R. Ramli, "Minimum mean brightness error bi-histogram equalization in contrast enhancement," IEEE Transactions on Consumer Electronics, vol. 49, pp. 1310-1319, 2003.
[29] C. Wang and Z. Ye, "Brightness preserving histogram equalization with maximum entropy: a variational perspective," IEEE Transactions on Consumer Electronics, vol. 51, pp. 1326-1334, 2005.
[30] C. H. Ooi, N. S. P. Kong, and H. Ibrahim, "Bi-histogram equalization with a plateau limit for digital image enhancement," IEEE Transactions on Consumer Electronics, vol. 55, pp. 2072-2080, 2009.
[31] P. Marziliano, F. Dufaux, S. Winkler, and T. Ebrahimi, "A no-reference perceptual blur metric," in Image Processing. 2002. Proceedings. 2002 International Conference on, 2002, pp. III-57-III-60 vol. 3.
[32] A. Grigoyan and S. Agaian, "Image Enhancement," in Advances in Imaging and Electron Physic, ed: Academic Press, May 2004, pp. 165-243.
[33] W. M. Morrow, R.B.Paranjape, R. M. Rangayyan, and J. E. L. Desautels, "Region-based contrast enhancement of mammograms," IEEE transactions on Medical Imaging vol. 11, pp. 392-406, Sep. 1992.
[34] E. Peli, "Contrast in complex images," Journal of Optical Society of America, vol. 7, October 1990.
[35] S. S. Agaian, "Visual morphology," in Electronic Imaging, 1999, pp. 139-150.
[36] S. DelMarco and S. Agaian, "The design of wavelets for image enhancement and target detection," Mobile Multimedia/Image Processing, Security, and Applications, pp. 735103-12, 2009.
[37] K. Panetta, S. Agaian, Y. Zhou, and E. Wharton, "Parameterized logarithmic framework for image enhancement," IEEE Transactions on Systems, Man, and Cybernetics—Part B: Cybernetics, vol. 41, April 2011.
[38] E. Wharton, S. Agaian, and K. Panetta, "Comparative study of logarithmic enhancement algorithms with performance measure," in Electronic Imaging, 2006, pp. 606412-606412-12.
[39] G. Buchsbaum, "An analytical derivation of visual nonlinearity," IEEE Transactions on Biomedical Imaging, vol. BME-27, pp. 237-242, 1980.
[40] N. Ponomarenko, et al., "Color image database for evaluation of image quality metrics," in Multimedia Signal Processing, 2008 IEEE 10th Workshop on, 2008, pp. 403-408.
[41] I. Lawrence and K. Lin, "A concordance correlation coefficient to evaluate reproducibility," Biometrics, pp. 255-268, 1989.
[42] J. B. Carroll, "The nature of the data, or how to choose a correlation coefficient," Psychometrika, vol. 26, pp. 347-372, 1961.

BIOGRAPHIES

Karen Panetta ((S'84–M'85–SM'95–F'08) received the B.S. degree in computer engineering from Boston University, Boston, MA, and the M.S. and Ph.D. degrees in electrical engineering from Northeastern University, Boston. Dr. Panetta is currently a Professor in the Department of Electrical and Computer Engineering at Tufts University, Medford, MA, and Director of the Simulation Research Laboratory. She is the Editor-in-Chief of the IEEE Women in Engineering magazine. Dr. Panetta is the IEEE-USA Vice-President of Communications and Public Affairs. She also served as the 2011 chair of the IEEE Boston Section, which has over 8800 members. During 2007 to 2009, she served as the world wide Director for IEEE Women in Engineering, overseeing the world's largest professional organization supporting women in engineering and science. Her research focuses on developing efficient algorithms for simulation, modeling, signal, and image processing for biomedical and security applications. She is a Fellow of the IEEE. She is also the recipient of the 2012 IEEE Ethical Practices Award and the Harriet B. Rigas Award for Outstanding Educator. In 2011, Dr. Panetta was awarded the Presidential Award for Engineering and Science Education and Mentoring by U.S. President Obama.

Chen Gao (S'10) received the B.S degree in Electrical Engineering from Beijing Normal University, Beijing, China in 2008 and the M.S in Electrical and Computer Engineering from Polytechnic Institute of NYU in 2010. Her research interests include image contrast enhancement, color enhancement, edge detection and color image quality assessment. She is a student member of IEEE, WIE and SPIE**.**

Sos Agaian (M'98–SM'00) is Peter T. Flawn Professor of Electrical and Computer Engineering at the University of Texas, San Antonio, and Professor at the University of Texas Health Science Center, San Antonio. Dr. Agaian received the M.S. degree (summa cum laude) in mathematics and mechanics from Yerevan University, Armenia, the Ph.D. degree in math and physics from the Steklov Institute of Mathematics, Russian Academy of Sciences, and the Doctor of Engineering Sciences degree from the Institute of the Control System, Russian Academy of Sciences. He has authored more than 500 scientific papers, 7 books, and holds 14 patents. He is a Fellow of the International Society for Photo-Optical Instrumentations Engineers, a Fellow of the Society for Imaging Science and Technology(IS&T), and a Fellow of the Science Serving Society (AAAS). He also serves as a foreign member of the Armenian National Academy. He is the recipient of MAEStro Educator of the Year, sponsored by the Society of Mexican American Engineers and Scientists. The technologies he invented have been adopted across multiple disciplines, including the US government, and commercialized by industry. He is an Editorial Board Member of the Journal of Pattern Recognition and Image Analysis and an Associate Editor for several journals, including the Journal of Electronic Imaging (SPIE, IS&T) and the System Journal (IEEE). His research interests are Multimedia Processing, Imaging Systems, Information Security, Artificial Intelligent, Computer Vision, 3D Imaging Sensors, Signal and Information Processing in Finance and Economics, Biomedical and Health Informatics.